American Journal of Nano Research and Applications
2017; 5(2): 19-31
http://www.sciencepublishinggroup.com/j/nano
doi: 10.11648/j.nano.20170502.12

Laser Technologies in Spintronics and Nanoelectronics as the Method of Changing the Structure and Magnetic Characteristics of Thin Films

Mykola M. Krupa

Department of Magnetic Nanostructures, Institute of Magnetism National Academy of Sciences and Ministry of Education and Science of Ukraine, Kiev, Ukraine

Email address:
krupa@imag.kiev.ua

To cite this article:
Mykola M. Krupa. Laser Technologies in Spintronics and Nanoelectronics as the Method of Changing the Structure and Magnetic Characteristics of Thin Films. *American Journal of Nano Research and Applications.* Vol. 5, No. 2, 2017, pp. 19-31.
doi: 10.11648/j.nano.20170502.12

Received: March 21, 2017; **Accepted**: April 22, 2017; **Published**: June 3, 2017

Abstract: In the present article we want to consider some features of not thermal influence of laser pulses on multilayer heterogeneous nanofilms to present the results of our experimental researches of change of the roughness of a surface and magnetic characteristics of permalloy films after their irradiation nanosecond laser pulses and the results of measurement of dynamics of magnetic reversal of magnetic tunnel nanostructures with one and two magnetic nanolayers. It is shown that the photon drag effect of electrons can not only generate an electric potential difference between the input and output surfaces in a semiconductor, but may also lead to a drift of the impurities. The results of our research show that in the thin CdS single crystals can be obtained stimulated emission of electromagnetic radiation in the terahertz frequency range.

Keywords: Multilayer Magnetic Nanofilms, Laser Pulses, Photon Drag Effect, Magnetic Reversal of Nanofilms, Spin Current, Spintronic, Terahertz Radiation

1. Introduction

Over fifty years of its existence, lasers have gone from the invention through the rapid development of lasers as a technique for widespread use in research, industry, medicine, metrology, data recording and processing, military engineering and even in art. Studies of laser interaction with matter, not only has put basis of laser materials processing technologies [1, 2], but also allowed to open several new physical effects, such as the laser-induced orientation of electron spins, photon drag effect in solids [3, 4], photon pressure, the drift of particles under laser irradiation [5], cooling of atoms in laser field [6], and laser-induced drift of atoms in the gas mixture [7], etc. Many of these effects are already widespread used today, for instance, for surface treatment and alloying of the surface layer in mechanical engineering and microelectronics, the isotope separation, frequency standards. However, not all possibilities of laser technology are well enough understood and used in practice.

The last assertion with good reason can be attributed to such areas of science and technology as nanoelectronics and spintronics. The base material for nanoelectronics and spintronics are multilayer nanofilm structures. The laser beam passes through several layers of ultra-thin films, and non-thermal effects play an important role in its interaction with such materials. The widest range of non-thermal effect of laser radiation mechanisms exist for magnetic nanofilms, which are the basic material for spintronics elements. Spintronics is a field microelectronics, which is based on the transport processes of spin-polarized current between the elements of electronic devices. Manipulation by the spin currents assumes using efficient spin current sources (injectors), control unit device by an electron spin direction and spin filtering. The main efforts of researchers and technologists working in the field of spintronics aimed at searching for magnetic materials with a high degree of spin polarization. At room temperatures there is predominant orientation of electron spins in ferromagnetic metals (FM), magnetic semimetals and magnetic semiconductors. For the latter the spin polarization degree at the Fermi surface can reach 100% [8, 9].

Obviously, in the production of spintronic elements the

problem arises concerning the adaptation of using materials to existing microelectronic technology. Majority of the known half-metallic magnetic alloys are complex compounds and technology of their production is complicated enough. Widely used in microelectronics generally non-magnetic semiconductors such as silicon, gallium arsenide and germanium under magnetic impurity doping are characterized by in homogeneities in the form of clusters.

For spin current control in spintronics devices it is necessary to change the state of magnetization of control and spin filter elements. It is necessary to understand, that the devices of spintronics can replace similar devices of microelectronics in enough limited area of technology. First of all, it is the area of registration and processing of small constant and super-high-frequency electromagnetic signals. For such signals elements of spintronics based on metallic nanostructures are compared to the semiconductor elements of microelectronics more low noise, high thermal stability factor and can be used in a higher frequency range. For creation of super-high-frequency devices of spintronics it is necessary to change the state of magnetization of control and spin filter elements with super-high-frequency. It is understood that the material of the electrodes must remagnetizing at high speed. Study the dynamics of the spin relaxation processes in solids and development of methods for active control of spin spin-polarized current in solid-state circuits constitute the main directions of the spintronics.

High sensitivity of magneto-optical polarization methods of measurement, methods of measurement, a change of pulse duration (from nanosecond to femtosecond) of laser pulses and sharp focusing of radiation all it allows to consider laser methods as one of the best not only at the studying of dynamics of switching of magnetic films, but also at use in technology of nanoelectronics and spintronics.

In the present article we want to consider some features of not thermal influence of laser pulses on multilayered heterogeneous nanofilms to present the results of our experimental researches of change of the roughness of a surface and magnetic characteristics of permalloy films after their irradiation nanosecond laser pulses and the results of measurement of dynamics of magnetic reversal of magnetic tunnel nanostructures with one and two magnetic nanolayers. We hope that these results will be useful to researchers and technologists to experts at studying of spin- dependent conductivity in magnetic materials and by working out of technology of new high-speed elements of spintronics.

2. Modification of Magnetic Characteristics of Polycrystalline NiFe Films at the Irradiation Laser Pulses

At thermal processing of laser materials use in most cases their warming up to temperature above the melting temperature. The question of influence of laser radiation on mechanical, electric and magnetic characteristics of materials at heating below fusion temperature investigated weakly. He cannot be considered for thin films as very important and especially for magnetic films. Such method of processing of thin films allows to change locally, in most cases allows to improve in most cases technical characteristics of elements nanoelectronics and spintronics.

Therefore, we conducted experimental studies of the interaction of nanosecond pulses of Nd:YAG laser (λ=1064 nm, τ=30 ns and λ=355 nm, τ=15 ns) with Gaussian distribution of energy in cross section and pulses of excimer laser (λ=248 nm,τ= 20 ns) with polycrystalline NiFe films. In electronics and spintronics elements the polycrystalline films are used in most cases, and the basic characteristics of NiFe films are well studied. They have a high permeability and low coercive force, but their coercive force Hc and magnetic susceptibility pretty much depend on the structure and internal stresses. Therefore polycrystalline NiFe films are good model for research of features of interaction of laser radiation with magnetic metal films at the intensity of radiation which is much less the intensity of the melting of this film.

We investigated nanocrystalline $Ni_{81}Fe_{19}$ film with thickness 0.25 and 0.5 microns, and a dual layer NiFe film with thickness of each layer 20 nm. The film was deposited on a substrate of polycrystalline silicon and fused silica.

The results of our researches have shown what even one powerful laser pulse causes a change of characteristics of $Ni_{81}Fe_{19}$ film in the irradiation zone. The roughness of a surface of a film decreases and also increases its magnetic permeability and its coercive force decreases. And appreciable changes of characteristics of $Ni_{81}Fe_{19}$ film are observed even after action of a nanosecond laser pulse which energy is insufficient for a heating of the film to melting temperature.

Figure 1 shows the results of changing the surface roughness of the NiFe film after irradiation with one pulse Nd-YAG laser (λ=1064 nm) and excimer laser focused pulse cylindrical lens (λ=248 nm). The irradiation of excimer laser sample was moved after each pulse at 250 μ. The surface of the film after irradiation becomes smoother, and the loop region with a low roughness section coincides with the contour of the laser beam on the surface. Interesting changes of the surface (Figure 1 – 4) were observed after irradiating pulses of the films of the third harmonic of Nd:YAG laser (λ=355 nm, τ=15 ns) with Gaussian distribution of energy in cross section. On the surface of the film structure at a high radiation intensity a little less film damage threshold is observed

Irradiation of even a single laser pulse results in substantial changes in the magnetic characteristics of $Ni_{81}Fe_{19}$ film. The switching curve becomes narrow and rectangular (Figure 2). At a low energy density of the laser pulse (less than W=0,1 J/cm^2) the film characteristics change little. With the increased energy density of laser pulse magnetic permeability μ increases and coercive force of the film H_c decreases. For the pulses with a high energy density (on the damage threshold of the film), these magnetic properties change less. The maximum amount of change in the magnetic characteristics of the films depends on the laser photon energy. For the film of 500 nm thick at magnetic susceptibility μ for Nd:YAG laser at λ=1,064 nm increased

almost 3 times, and the coercive force H_c decreased about two. For the excimer laser at λ=248 nm, we have received an increase in the magnetic susceptibility μ almost ten times while a decrease in coercive force H_c was 5 times. Similar changes in the magnetic characteristics are observed in the films irradiated by pulses of the third harmonic Nd:YAG laser (λ=355 nm, τ=15 ns).

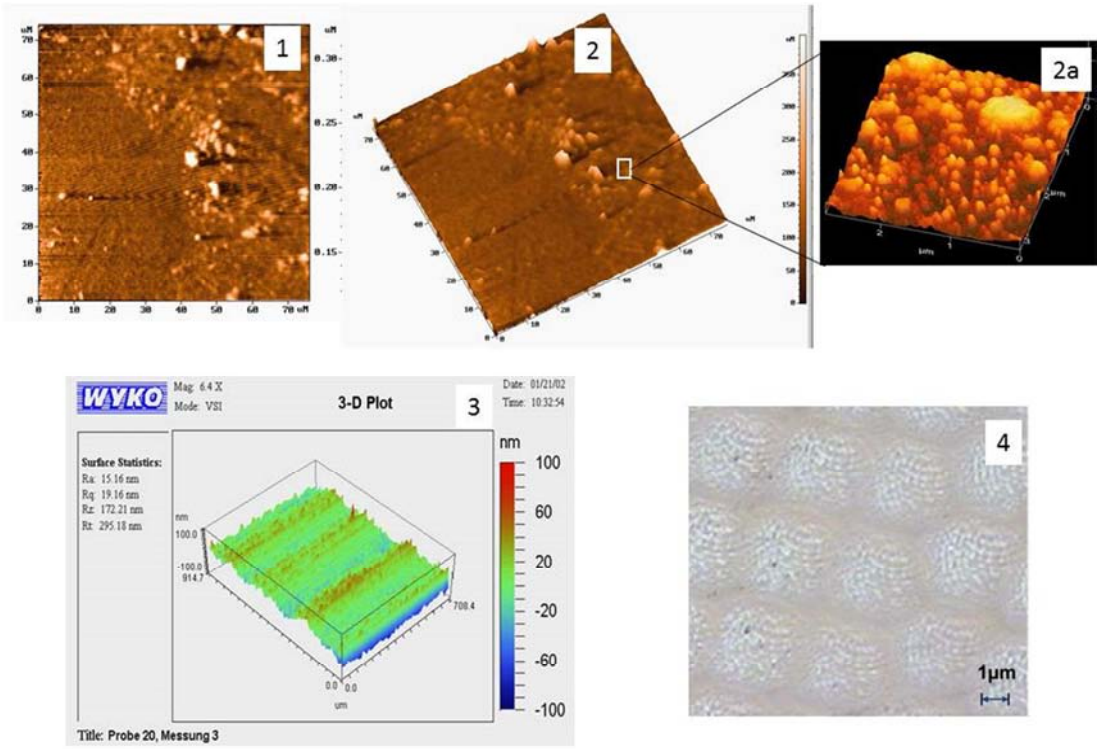

Figure 1. *Change in the roughness of surface of $Ni_{81}Fe_{19}$ film after irradiation with one pulse Nd-YAG laser (1, 2, 4 – spherical lens, 2a - enlarged image) and excimer laser (3 – cylindrical lens).*

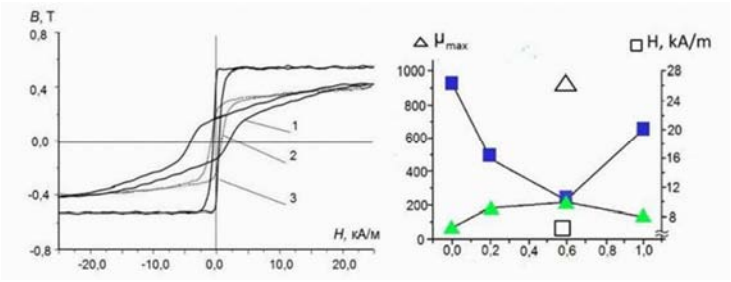

Figure 2. *Change of the form of the switching curve (I), and also magnetic permeability μ and coercive force H_c (II) in film $Ni_{81}Fe_{19}$ with the thickness of 500 nm after an irradiation nanosecond laser pulses: I-1 –switching curve loop of magnetic reversal to an irradiation, I-2 –pulse of Nd:YAG laser (λ=1064 nm), W=0,6 J/cm^2; I-3 –pulse of excimer laser W=0,6 J/cm^2; II-1 –pulse of Nd:YAG laser (λ=1064 nm) at different density of energy, II-2 – pulse of excimer laser W=0,6 J/cm^2.*

The maximum amount of change in the magnetic characteristics of the films depends on the laser photon energy. For the film of 500 nm thick at magnetic susceptibility μ for Nd: YAG laser at λ=1,064 nm increased almost 3 times, and the coercive force H_c decreased about two. For the excimer laser at λ=248 nm, we have received an increase in the magnetic susceptibility μ almost ten times while a decrease in coercive force H_c was 5 times. Similar changes in the magnetic characteristics are observed in the films irradiated by pulses of the third harmonic Nd: YAG laser (λ=355 nm, τ=15 ns).

The initial temperature of the film (20°C to 300°C) has little effect on the relative magnitude of the change in its magnetic characteristics after irradiation by the laser pulse with the energy density W=0,6 J/cm^2. When the initial temperature of the film was 400°C its magnetic characteristics change little after irradiation. We observed analogous changes of magnetic characteristics in films $Ni_{81}Fe_{19}$ with thickness of 250 nanometers after an irradiation laser pulses. Distinction in change of magnetic characteristics was only that the size of the maximum change of a magnetic susceptibility and coercive forces was in such films more than the maximum size change of similar characteristics in films $Ni_{81}Fe_{19}$ with thickness of 500 nm.

Studies have shown that the composition of the film hardly varies after irradiation of the excimer laser pulses with density of energy W=0,6 J/cm^2, and changes only the nanocrystalline structure in a surface layer of a polycrystalline $Ni_{81}Fe_{19}$ film.

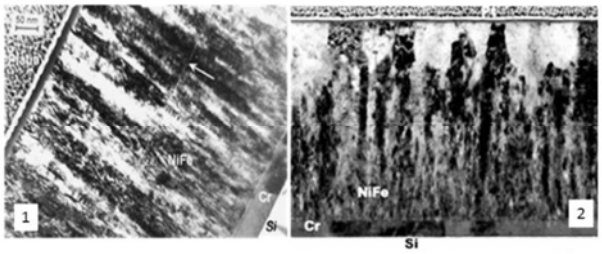

Figure 3. *Change of crystal structure of $Ni_{81}Fe_{19}$ film with a thickness of 500 nm after an irradiation one nanosecond pulse of excimer laser with density of energy W=0,6 J/cm^2: structure of cross-section section of the film to irradiation (1); structure of cross-section section after irradiation (2).*

It can be seen that, after irradiation, an increase in the size of the nanocrystals from the surface region of the laser pulse is observed. The value of such nanocrystals reaches 200-259 nm. We were not able to fix the crystal structure changes after irradiation pulse Nd-YAG (λ=1064 nm) laser. For the only samples we were able to pay, we could not detect any changes in crystal structure after irradiation pulse Nd-YAG (λ=1064 nm). It should be noted that on the damage threshold of film a regular structure appers after irradiation of 500 nm thick $Ni_{81}Fe_{19}$ uniform (Gaussian) beam of Nd-YAG laser (λ=355 nm and τ=15 ns) on the verge of destruction (melt) film on the surface of the film (Figure 1-4). The typical size of the structure element is about 200 nm, which makes it possible to connect it with a process of forming large nanocrystals.

Significant decrease of the roughness of surface shows that we have a melting or evaporation of needlelike nanoparticle on the surface of $Ni_{81}Fe_{19}$ film under laser pulses whose energy is insufficient to heat up to the melting point of the smooth surface of the film. This fact shows that we have a strong increase of the absorption of light or useful increase of the laser radiation field on such a needlelike nanoparticle of surfaces. This mechanism can be excitation of localized plasmon on the needlelike nanoparticle on the film surface. A plane wave does not excite the surface plasmons on the smooth surface of conductive film. However, the localized plasmons on metal nanoparticles are excited by light of any polarization. These plasmons increase the absorption of light and the intensity of electromagnetic field of light wave near to the surface [10]. The field E of the light wave excite in nanosphere with dielectric permeability ε_1 the wave of polarization $P=ER^3(\varepsilon_1-\varepsilon_0)/(\varepsilon_1+2\varepsilon_0)$ [3], where R – radius of curvature of the sphere, ε_0 – dielectric capacitivity in a medium.

The size of amplification coefficient η of electromagnetic field can be estimated on the basis of following expression [11].

$$\eta = \left(E_1 / E_0\right)^2 = \left(\varepsilon_0 / 3L^2\varepsilon_{12}\right)^2 \quad (1)$$

Where E_1 and E_0 –intensity of the field of incident wave and excited wave, $\varepsilon_1=\varepsilon_{11}+i\varepsilon_{12}$, L – geometric factor for metal particle. For an ellipsoid with eccentricity 3 it is equal L=0,1, and we will receive an useful increase of the size of amplification coefficient η.

In the field of falling of a laser beam on the film surface there is a big number of needlelike nanoparticles. All these needlelike nanoparticles are excited by laser radiation coherently. As a result, there is a considerable strengthening of the electromagnetic field of laser radiation at the expense of folding weeding excitation of all particles. For two particles on distance r amplification coefficient η will register as

$$\eta = \left|\frac{B}{1-\alpha_1\alpha_2 A^2}\left(\alpha_1 + 2\alpha_1\alpha_{21}A + \alpha_2\right)\right|^2 \quad (2)$$

If two particles contact, the expression for amplification coefficient is possible to be written down as [11]

$$\eta = \left|\frac{16(\varepsilon_{12}-1)}{3(\varepsilon_{12}+3)}\right|^2 \quad (3)$$

Where $\alpha=R^3\varepsilon_0(\varepsilon_{12}-\varepsilon_0)/3[\varepsilon_0+L_i(\varepsilon_{12}-\varepsilon_0)]$; $A=(r^{-3}+ikr^{-2})e^{-ikr}$; $B=2(8r^{-3}+i4kr^{-2})e^{-ikr/2}$.

This expression shows that amplification coefficient η is much bigger then 1 (η>>1). At the big intensity of laser radiation it is necessary to consider the nonlinear response in the polarizability of particles that will lead to a big increase of amplification coefficient η.

All stated above shows that localized on the needlelike nanoparticle plasmons play important role in processes of interaction of laser radiation with the surface of metal films. Such localized plasmons are a source of increase of the coefficient of absorption and cause the amplification of a field of laser radiation falling on the film surface. These processes can reduce the surface roughness of the film by laser radiation without damage to the film surface.

Our researches show, that not thermal processes play also the important role at the change of magnetic characteristics of $Ni_{81}Fe_{19}$ films under the action of laser pulses. That confirmation of this is quite a strong dependence of the efficiency of these processes from the laser photon energy. Laser pulse heating the film also influences the efficiency of the polycrystalline structure and magnetic characteristics. We also believe that the efficiency of the recrystallization of the surface layer of the film depends on the degree of ionization of an atoms in the laser radiation zone. The results show that the depth of the recrystallization of the film coincides well with the depth of the penetration of laser radiation in the film $Ni_{81}Fe_{19}$. The measured values of the absorption coefficient k up to the excimer laser at λ=248 nm $k=(3-6)\times10^4$ cm^{-1} and for the Nd:YAG laser at λ=1064 nm $k=(2-4)\times10^5$ cm^{-1}. The

photon energy for the excimer laser is three times more the photon energy of the Nd:YAG laser. Therefore, the thickness of the layer of ionized $Ni_{81}Fe_{19}$ film and the degree of ionization of atoms is much more to the excimer laser than for Nd: YAG laser. This factor is the determining factor in the process of recrystallization and and change the magnetic characteristics of the film under the action of nanosecond laser pulses.

On recrystallization processes in the ionized layer of the film may also influence photon drag effect. The physical mechanism of this phenomenon will be discussed below.

3. Photon Drag Effect and Drift of Ionized Atoms in Multilayer Nanofilms

The photon drag effect was experimentally detected in semiconductor crystals [3, 4]. This effect is due to the transfer of a photon to an electron pulse, which leads to the direction of motion of the electrons in the direction of propagation of the laser beam. The value of such the laser stimulation current can be found from the following expression [3, 12, 13]

$$j = -(1-R)e\alpha I \frac{n_0 \tau_p \gamma}{m_e c}, \qquad (4)$$

where e and m_e are the charge and effective mass of an electron; c is the velocity of light; n_0 is the refractive index of the semiconductor; I, ω R and α are the intensity, frequency, reflection and absorption coefficient of laser radiation; τ_p is averaged electron momentum relaxation time in the conduction band; γ is numerical factor less than unity, which defines the momentum transfer of photons by electrons.

This laser stimulation current creates a high concentration of non-equilibrium electrons N_e in the laser beam exit area.

$$N_e \approx (1-R)\alpha I \frac{2\pi n_0 \tau_p \gamma}{h\omega} \qquad (5)$$

The electrostatic interaction of charge of these non-equilibrium electrons with the charged ionized atoms can cause their directed moving. Energy of electrostatic interaction We of the ionized atom with the field of spatial charge of non-equilibrium electrons is proportional to their concentration of Ne, and approximately inversely proportional to distance of the charged atom from the center of charge of non-equilibrium electrons l.

$$W_e \approx N_e S_0 l_0 \frac{\varepsilon e^2}{4\pi\varepsilon_0 l} \approx (1-R)\alpha l e^2 \frac{n_0 r_0^2 l_0 \tau_p \gamma}{2\varepsilon_0 \varepsilon h\omega l} \qquad (6)$$

Here $S_0=\pi r_0^2$ –area of section of laser beam; $l > l_0$, l_0 – thickness of area of localization of space charge of non-equilibrium electrons. Even at the not high levels of intensity of laser radiation I=1 kW/cm^2, $\omega = 10^{14} c^{-1}$ $\alpha = 10^4$ cm^{-1}, $\varepsilon = 4$, $R=0,5$, $r_0=0,5$ cm, $\tau_p=10^{-10}$-10^{-11} s, $l_0=0,0l$, $\gamma=0,5$ we will get for energy of electrostatic interaction of the singly ionized atom the high values $W_e>100$ eV. It is understood that the expression (6) is an approximation, but it shows that the energy of the electrostatic interaction of ionized atoms from the space charge of non-equilibrium electrons can cause a drift of these atoms in the direction of the laser pulse.

Experimental researches of interaction of laser radiation with different materials show that under the action of short laser pulses even in metals there is an effective transfer of impurity atoms from a surface in a depth material [14, 15]. Our researches [16] of the films dye-bismuth-dye and SiC-Bi-SiC, consisting of three sequentially deposited nanolayers with a thickness of individual layers 6-8 nm, showed that after irradiation of such a structure by the laser pulses bismuth atoms move along the laser beam. In these films the phthalocyanine dye layers is virtually transparent to laser light, and a layer of bismuth absorbs strongly. We also studied the influence of nanosecond excimer laser pulses on diffusion processes in in the two-layer Ni-Fe film.

After irradiation nanosecond laser pulse in such two-layer and three layer films there is an asymmetric change in concentration of atoms of bismuth, iron, and nickel (Figure 4). The concentration of the bismuth atoms increases under the influence of laser radiation in the output layer, and also does not change in an entrance layer almost any change in the input layer of the semiconductor or dye. The measurement results show that under the influence of the laser pulse observed the asymmetry in the diffusion of iron and nickel atoms. The diffusion of atoms Ni and Fe in the direction of the laser pulse is much stronger.

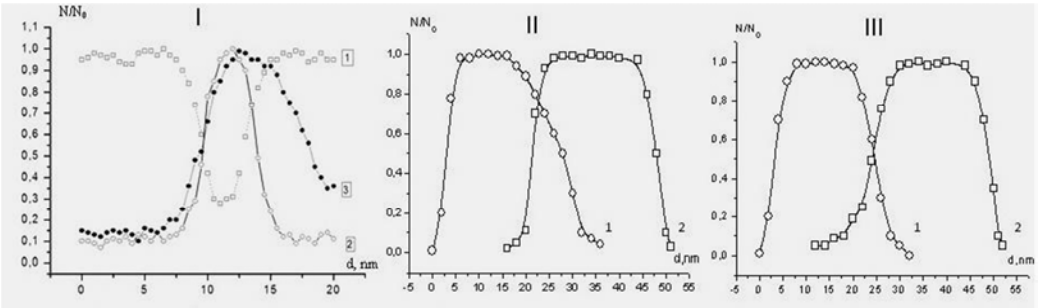

Figure 4. *Distribution of atoms of bismuth in the three-layer film of phthalocyanine dye-bismuth-dy.*

(I) and atoms Ni and Fe in the two-layer Ni-Fe film after the irradiation of ruby laser pulse ($\tau_i=20$ ns) (I) and excimer

laser pulse (τ_i=*20 ns*) with the energy density W=0.6 J/cm^2 (II – film irradiated from nickel layer and III – film irradiated from iron layer): I-1 – the dye concentration, I-2 – the concentration of bismuth prior to the irradiation, I-3 – the bismuth concentration after irradiation; II-1and III-1 – the concentration of Ni, II-2 and II-2 – the concentration of Fe.

Based on these results it can be argued that a powerful laser pulses cause the directional drift of bismuth and iron or nickel atoms. In our opinion, such a laser stimulated drift of atoms caused by electrostatic interaction of ionized atoms with the field of space charge of the electrons, which appears at the output of the laser beam due to the photon drag effect. The above experimental results show that the photon drag effect plays an important role in the interaction of laser radiation with heterogeneous multilayer nanofilms and can be used for doping semiconductor nanofilms. This technology can be successfully used in spintronic to create the homogeneous magnetic semiconductor films, which have the photon drag effect high degree of spin polarization of the conduction electrons.

4. Excitation of a Spin Current and the Switching of Magnetic Films by Laser Radiation

In the two-layer magnetic nanofilms the photon drag effect can cause not only a well-known electric current, but cause the appearance of spin current. If the first magnetic nanolayer there is a high spin polarization of the conduction electrons (such as 100%) under the action of intense laser radiation, they are injected into the second layer (magnetic or nonmagnetic) and in such a structure is excited spin current. The spin-polarized electrons are accumulated on a spin free path in the second nanolayer and a complementary magnetization arises in the nonmagnetic layer [30]. The spin free path $l_s = \upsilon_p \tau_s$, where τ_s is the character relaxation time of the spin polarization, $\upsilon_p = hk/2\pi m_e^*$ is the velocity of laser-injected electrons, $hk/2\pi$ is the laser photon pulse, m_e^* is the electron effective mass. The spin relaxation time of polarized electrons in a nonmagnetic material more than the momentum relaxation time $\tau_s > \tau_p$. We will receive for an estimation of size of nonequilibrium magnetization created laser-induced spin current following expression

$$M_s \approx A\mu_B N_{es} V_{es} \approx A(1-R)\alpha\mu_B I \frac{\pi n_0 r_0^{\,2} \tau_s \tau_p \gamma \xi}{cm_e} \qquad (7)$$

Here r_0 is the radius of the laser beam, V_{es} is the volume of localization, ξ<1 is the coefficient characterizing the efficiency of the electron transmission through the interface between two layers, A is coefficient of proportionality,. Estimates of the average velocity, density and mean free path of spin polarized electrons injected into the nonmagnetic layer show that even at not very high laser intensity $I=10^5 W/cm^2$, photon energy $h\nu$ =*1eV,* α =10^4-10^5 cm^{-1}, $R=0,5$, $\tau_s=10^{-9}$ *s*, $\xi=0,8$, and $\gamma=0,8$. Therefore these values reach high values: $v_e \sim 10^5$ *cm/s,* $l_s \sim 10^3$*nm,* $N_{es} = 10^{19}$-10^{18} cm^{-3}.

A similar magnetization was first observed in measurements of electrical conductivity of bilayer structures ferromagnetic-nonmagnetic metal [17]. Experimental studies of nonequilibrium polarized electrons which are laser-excited in the non-magnetic layers in the above mentioned magnetic nanostructures are a complicated enough problem. This is related to a small lifetimes and quantity of the total magnetic moments because of the small volumes V_{es}. Therefore, experimental measurements assume such methods, which allow to detect a weak signal against the background of strong noise signals. One of the best methods of solving this problem is to use magneto-optical measurement techniques. Measurements of magneto-optical Kerr and Faraday angles allow to obtain high sensitivity and provide an opportunity to measure these angles in small local regions with a high speed. The values of additional angle of the polarization twisting, corresponding to the laser-induced drift, at a given laser intensity can be obtained by numerical calculations an. These calculations assume the experimental determination of the parameters of the multilayer film nanostructures.

We can conclude [18] that the magnitude of the additional nonequilibrium Kerr angle φ_e in the nonmagnetic layer is proportional to the ratio of the concentration N_{es} of the laser-excited polarized nonequilibrium electrons to the concentration of equilibrium electrons N_0. The magnitude of the additional nonequilibrium Faraday angle θ_e its proportionality to the nonequilibrium magnetization M_s and thickness of a magnetic medium.

$$\varphi_e \approx A\chi(\omega)\frac{N_{es}}{N_0};\ \theta_e = AKM_s l_s = (1-R)\alpha\mu_B AIKl_s \frac{\pi n_0 r_0^{\,2} \tau_s \tau_p \gamma \xi}{cm_e} \qquad (7)$$

Here $\chi(\omega)$ is magneto-optic coefficient, K is the Hund constant, N_0 is the concentration of equilibrium electrons, l_s is the thickness, A is a proportionality coefficient.

Laser radiation can cause the switching of magnetic films at the expense of thermal and not thermal mechanisms of magnetic reversal. Heating of a film and the reduction of force of a magnetic film and its switching under the influence of an external magnetic field or the field of demagnetization is the basic thermal mechanism of magnetic reversal. The time of this thermal laser action is determined by the spin-electron and spin-phonon relaxation times and lies on the nanosecond time scale. Such a mechanism of magnetic reversal is well-known and also is widely used for magneto-optical recording in ferrimagnetic films [19].

High speed laser-induced thermal magnetization reversal obtain in the film with the antiferromagnetic structure, which have the opposite orientation of the magnetization of the magnetic sublattices [20, 21]. These magnetic sublattices have various the speed of switching and size of factor of thermal reduction of the magnetic moment. At cooling of this film its switching occurs under the influence of an internal magnetic field and a field of of antiferromagnetic exchange interaction in the magnetic sublattices.

Non-thermal switching of magnetic films by laser

radiation can occur due to the inverse Faraday effect [22, 23] or the injection of spin-polarized electrons induced by this radiation [23]. The laser beam with circular polarization generates in the film by the inverse Faraday effect the nonequilibrium magnetic moment, which is directed in the direction of propagation of the radiation, and the magnitude of which is proportional to the square of the field intensity of the light wave.

$$\overrightarrow{M}_F = \frac{\chi}{16\pi}\left[\vec{E}\times\overrightarrow{E^*}\right] \quad (8)$$

χ is the magneto-optical susceptibility of the medium. This mechanism is realized only at the circular polarization of laser radiation and the created magnetic field H_F. The magnitude of the field in the thin conductive films can be found on the basis of a circular current laser-induced [23].

$$H_F = \frac{\left|\overrightarrow{M}_F\right|\mu}{4\pi\mu_0} = \frac{e^3\mu NE^2}{16\pi\mu_0 n(m_e^*)^2\omega^3} = \frac{e^3\mu NI}{8\pi\mu_0 c\varepsilon_0 n(m_e^*)^2\omega^3} \quad (9)$$

Where ω is a laser frequency; c is light speed; m_e* and N are effective masse and concentration of conductive electrons; ε , μ are dielectric and magnetic constant. The direction of the magnetization vector varies with the direction of rotation of the field vector of circularly polarized electromagnetic radiation on the opposite. The calculated value of laser-induced internal magnetic field can reach large values H_F>10^5–10^6 A/m for magnetic films with μ =10^3-10^4 and $N \approx 10^{22}$ cm^{-3} under relatively low radiation intensity of picosecond or femtosecond laser pulses I=10^9 W/cm^2. The characteristic relaxation time for the inverse Faraday effect is equal 10^{-13} s (10).

The switching of the second and next magnetic layer can pass in multilayered magnetic nanostructures under the influence of the spin polarized electrons which are injected into the layer by laser radiation [24]. The spin polarized electron produces a nonequilibrium magnetic field H_i. This field consists of a field of electric current H_e and the magnetic field H_s related to the total magnetic moment of the injection spins H_i=H_e+H_s [14]. These magnetic fields have different directions: the field produced by electric current H_e lies in the plane of the film, while the field of the total spin moment of the electrons injected from the first magnetic layer H_s is directed along the magnetization M_1 of the first magnetic layer. The results of the article [15] showed that the relation H_e /H_s~d_0 (d_0 is the diameter of the current conductor).

The magnetic field He and Hs have is proportional to the injection current density arising under the influence of laser radiation. From the expression (4) can be written [25]

$$H_e = l_e\alpha(1-R)Ier\frac{n_0\tau_p\gamma\xi}{4\pi m_e c}\ H_s = l_s\alpha(1-R)I\mu_B\mu\frac{n_0\tau_p\tau_s\gamma\eta\xi}{2\mu_0 h_2 m_e c} \quad (10)$$

where I, α and R and also n_0 are an intensity, absorption and reflection coefficients, and also refractive index of laser radiation falling on the first magnetic layer, respectively; r is the radius of a laser beam, h_1 and m_e are the thickness of the first magnetic layer and effective electron mass; c is a light speed; γ<1, η <1 and ξ <1 are coefficients characterizing a momentum transfer from photons to electrons in the first magnetic layer and the degree of an electron polarization and affectivity of the electron passage from the first into the second layer; μ_B is the Bohr magneton; μ and μ_0 are the a magnetic and absolute magnetic permeability; l_s and l_e are proportionality constant. At I=100 MW/cm^2, α=10^5 cm^{-1}, R=0,5, r=10^{-6} m, τ_s=10^{-10}-10^{-11} s, τ_p=10^{-11}-10^{-12} s, μ =10^4, γ=0,8, η=0,8, ξ =0,5 we can obtain the value H_s>10^6 A/m and H_e =10^4-10^5 A/m. Thus theoretical estimates have shown that the laser-induced spin-polarized current can causes the magnetic switching of magnetic layers with perpendicular and planar uniaxial magnetic anisotropy.

The dynamics of variation of magnetic moment $\overrightarrow{M}$ can be described with the help of the Landau–Lifshitz-Gilbert equation of the form

$$\frac{d\vec{M}}{dt\overline{\overline{M_o}}} = \gamma\left[\frac{\vec{M}}{\overline{\overline{M_o}}}\times\vec{H}\right] + \frac{\gamma\alpha_{\parallel}}{n^2}\left[\frac{\vec{M}}{\overline{\overline{M_o}}}\times\vec{H}_{eff}\right]\frac{\vec{M}}{\overline{\overline{M_o}}} - \frac{\gamma\alpha_{\perp}}{n^2}\left[\frac{\vec{M}}{\overline{\overline{M_o}}}\times\left[\frac{\vec{M}}{\overline{\overline{M_o}}}\times\vec{H}_{eff}\right]\right], \quad (11)$$

Here M=$f(T)$ and M_0=$M(T$=0); $\alpha_{//}$ and $\alpha_{\perp}$ are coefficients of a longitudinal and cross-section relaxation, γ-is a coupling factor. The effective magnetic field can be represented as the sum $\vec{H}_{eff} = \vec{H}_{ext} + \vec{H}_{an} + \vec{H}_F + \vec{H}_i + \vec{H}_{dm}$, where H_{ext} is the external magnetic field, H_{an} is the coercive forcer, H_F is the magnetic field of inverse Faraday effect, H_i=H_e+H_s is the magnetic field of the laser-injected current and H_{dm} is the demagnetizing field. Through variation of the experimental conditions, it is possible to make any of these mechanisms predominant.

5. Switching the Conductivity of Tunnel Junctions and the Recording of Information on the Spin Media

We studied the dynamics of magnetization reversal of the magnetic single-layer nanofilms with perpendicular anisotropy $Tb_{25}Co_5Fe_{70}$ and $Tb_{19}Co_5Fe_{76}$ and nanofilms with uniaxial in-plane anisotropy $Co_{80}Fe_{20}$ and $Co_{30}Fe_{70}$ and the magnetic double-layer nanofilms $Tb_{22}Co_5Fe_{73}$ /Pr_6O_{11}/$Tb_{19}Co_5Fe_{76}$ and $Co_{80}Fe_{20}$/Pr_6O_{11}/$Co_{30}Fe_{70}$ under the action of nanosecond, picosecond and femtosecond laser pulses. At T=300 K the coercive forces of the layers $Tb_{22}Co_5Fe_{73}$ and $Tb_{19}Co_5Fe_{76}$ was equal $H_1 \approx 3x10^5$ A/m and $H_2 \approx 1,2x10^5$ A/m. The coercive force of the layers $Co_{30}Fe_{70}$ and $Co_{80}Fe_{20}$ was equal $H'_1 \approx 300$ A/m and $H'_2 \approx 800$ A/m. The magnetic nolayers in the investigated films were magnetized by the external magnetic field in the direction of the easy magnetization axis to a state near to a state of the saturation magnetization. The magnetic layers $Tb_{22}Co_5Fe_{73}$, $Tb_{19}Co_5Fe_{76}$, $Co_{30}Fe_{70}$ and $Co_{80}Fe_{20}$ in such state of the saturation magnetization have a sufficiently high degree of the spin polarization of electrons [26, 27]. The sputtering technique of the investigated nanofilms and their magnetic

characteristics are described in the article [26].

The magnetic switching of single-layer $Tb_{25}Co_5Fe_{70}$ and $Tb_{19}Co_5Fe_{76}$ films can be obtained without an external magnetic field for the circularly polarization of picosecond and femtosecond laser pulses and an external magnetic field, which is directed antiparallel to the initial magnetization of these films for any polarization and different duration laser pulses. The scheme of corresponding optical researching is represented in Figure 5.

The magnetic switching of single-layer $Co_{80}Fe_{20}$ and $Co_{30}Fe_{70}$ films can be obtained only in an external magnetic field, antiparallel to the initial magnetization of these films. In two-layer films $Tb_{22}Co_5Fe_{73}$ /Pr_6O_{11}/$Tb_{19}Co_5Fe_{76}$ and $Co_{80}Fe_{20}$/Pr_6O_{11}/$Co_{30}Fe_{70}$ the magnetic switching of the first nanolayer can be carried out in the same way as well as in single-layered films. The second magnetic nanolayer can be magnetized reversal also at the injection induced by laser radiation in this layer of the spin polarized electrons from the first magnetic layer that is we have the magnetization reversal by a spin current. However, such magnetization reversal of the second magnetic nanolayer it is possible only in that case when the coercive force of this layer is less than the coercive force of the first nanolayer and when the first and second layers are magnetized in opposite direction that is $Tb_{22}Co_5Fe_{73}\uparrow$/$Pr_6O_{11}$/$\downarrow Tb_{19}Co_5Fe_{76}$ and $Co_{80}Fe_{20}\uparrow$/Pr_6O_{11}/$\downarrow Co_{30}Fe_{70}$. If the both magnetic layers are magnetized in the identical direction ($Tb_{22}Co_5Fe_{73}\uparrow$/$Pr_6O_{11}$/$\uparrow Tb_{19}Co_5Fe_{76}$ and $Co_{80}Fe_{20}\uparrow$/Pr_6O_{11}/$\uparrow Co_{30}Fe_{70}$) then to make the magnetization reversal of a the layer $Tb_{19}Co_5Fe_{76}$ with the smaller coercive force it is possible under the influence of the circularly polarized laser pulse, and to make the magnetization reversal the layer $Co_{30}Fe_{70}$ it is possible only in an external magnetic field which is directed towards to the magnetization of this layer.

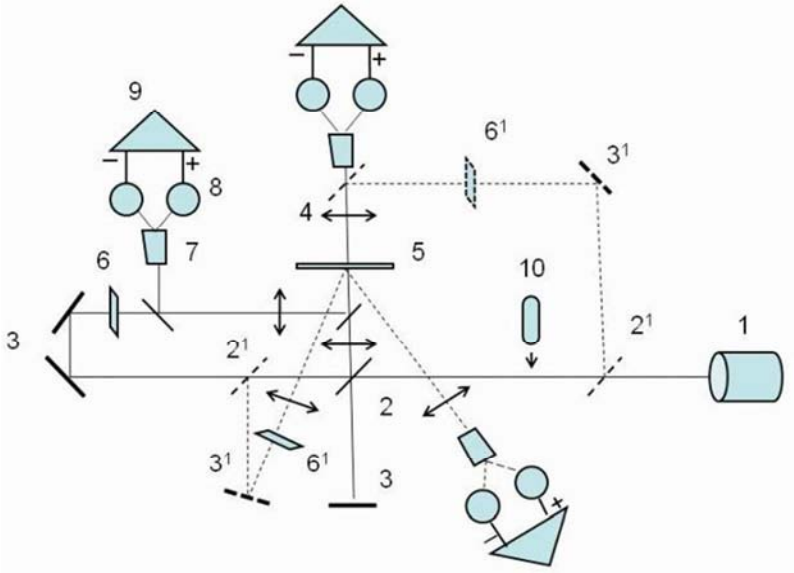

Figure 5. *Optical scheme of research of dynamic characteristics of magnetization reversal the films by laser radiation: laser –1, 50% mirror –2, total reflection mirror –3, long-focus lens –4, substrate with a film –5, polarizer –6, Senarmon prism –7, photodiode –8, differential amplifier –9, Babinet compensator –10.*

The magnetic switching of single-layer $Tb_{25}Co_5Fe_{70}$ and $Tb_{19}Co_5Fe_{76}$ films can be obtained without an external magnetic field for the circularly polarization of picosecond and femtosecond laser pulses and an external magnetic field, which is directed antiparallel to the initial magnetization of these films for any polarization and different duration laser pulses. The magnetic switching of single-layer $Co_{80}Fe_{20}$ and $Co_{30}Fe_{70}$ films can be obtained only in an external magnetic field, antiparallel to the initial magnetization of these films. In two-layer films $Tb_{22}Co_5Fe_{73}$ /Pr_6O_{11}/$Tb_{19}Co_5Fe_{76}$ and $Co_{80}Fe_{20}$/Pr_6O_{11}/$Co_{30}Fe_{70}$ the magnetic switching of the first nanolayer can be carried out in the same way as well as in single-layered films. The second magnetic nanolayer can be magnetized reversal also at the injection induced by laser radiation in this layer of the spin polarized electrons from the first magnetic layer that is we have the magnetization reversal by a spin current. However, such magnetization reversal of the second magnetic nanolayer it is possible only in that case when the coercive force of this layer is less than the coercive force of the first nanolayer and when the first and second layers are magnetized in opposite direction that is $Tb_{22}Co_5Fe_{73}\uparrow$/$Pr_6O_{11}$/$\downarrow Tb_{19}Co_5Fe_{76}$ and $Co_{80}Fe_{20}\uparrow$/Pr_6O_{11}/$\downarrow Co_{30}Fe_{70}$. If the both magnetic layers are magnetized in the identical direction ($Tb_{22}Co_5Fe_{73}\uparrow$/$Pr_6O_{11}$/$\uparrow Tb_{19}Co_5Fe_{76}$ and $Co_{80}Fe_{20}\uparrow$/Pr_6O_{11}/$\uparrow Co_{30}Fe_{70}$) then to make the magnetization reversal of a the layer $Tb_{19}Co_5Fe_{76}$ with the smaller coercive force it is possible under the influence of the circularly polarized laser pulse, and to make the magnetization reversal the layer $Co_{30}Fe_{70}$ it is possible only in an external magnetic field which is directed towards to the magnetization of this layer. The results of our experimental studies of the dynamics of magnetization reversal have shown that the time of magnetization reversal of our magnetic layers at the

irradiation their ultrashort laser pulse is less than 20 picoseconds (Figure 6).

It is necessary to notice that the measurements of time of the magnetic switching with the scheme shown on a Fig. 6 can give the overestimated values of time of the switching. To find the most exact values of time of switching it is necessary that diameter of cross-section section of the beam of the exciting laser pulse was much more than diameter of cross-section section of the beam of the test laser pulse and this the test laser pulse was focused precisely in the center of the beam of the exciting laser pulse.

We also investigated the effect of high-power laser pulses on the conductivity of the tunnel microcontacts $Tb_{19}Co_5Fe_{76}/Pr_6O_{11}/Tb_{22}Co_5Fe_{73}$ and $Co_{80}Fe_{20}/Pr_6O_{11}/Co_{30}Fe_{70}$. The tunnel microcontacts with a conductive surface $S\approx 20\ \mu^2$ are produced by a photolithography technique on the plates with sizes *10x14 mm*. The edge of plates through which the current was inputted to the tunnel contacts TbCoFe and CoFe is covered by platinum. The contact zone and conductive magnetic strips are also protected by the Al_2O_3 cover with thickness near 40 *nm*. Before measurements we carried out testing microcontacts with large and near tunnel resistances.

The research of the resistance of microcontacts $Tb_{19}Co_5Fe_{76}/Pr_6O_{11}/Tb_{22}Co_5Fe_{73}$ and $Co_{80}Fe_{20}/Pr_6O_{11}/Co_{30}Fe_{70}$ showed that at a small intensity of laser radiation the magnitude of resistance of contact falls at the moment of action of laser pulse, but then comes back practically to the initial value. In contacts $Tb_{22}Co_5Fe_{73}\uparrow/Pr_6O_{11}/\downarrow Tb_{19}Co_5Fe_{76}$ and $Co_{80}Fe_{20}\uparrow/Pr_6O_{11}/\downarrow Co_{30}Fe_{70}$ with magnetized in an opposite direction the magnetic layers it is possible to receive the switching of the conductivity of these contacts from a high-resistance state in a low-resistance state without a magnetic field under action only a laser pulse. What to receive such switching of conductivity it would be necessary to irradiate these contacts by a high-power laser pulses from the high-coercivity layers $Tb_{22}Co_5Fe_{73}$ or $Co_{80}Fe_{20}$.

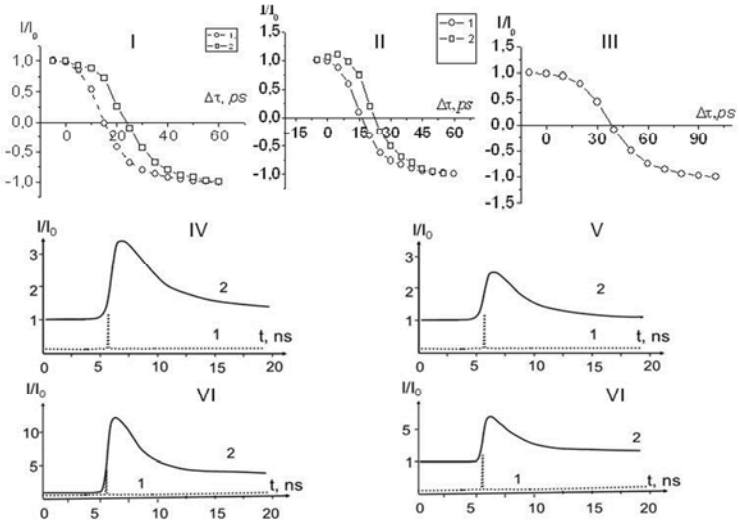

Figure 6. *The delay time curve (I-III) of a probe linearly polarized femtosecond laser pulses and the change of resistance of the tunneling contacts $Tb_{22}Co_5Fe_{73}\uparrow/Pr_6O_{11}/\downarrow Tb_{19}Co_5Fe_{76}$ (IV, VI) and $Co_{80}Fe_{20}\uparrow/Pr_6O_{11}/\downarrow Co_{30}Fe_{70}$ (V, VII) after an irradiation high-power femtosecond laser pulse: I –probe pulse passes through film $Tb_{19}Co_5Fe_{76}$ (1) and $Tb_{25}Co_5Fe_{70}$ (2); II –probe pulse is reflected from $Tb_{19}Co_5Fe_{76}$, high-power pulse has the circular polarization (1) and linear polarization (2); III – probe pulse is reflected from $Co_{30}Fe_{70}$, high-power laser pulse gets on the nanolayer $Co_{80}Fe_{20}$; T=300K (I -V) and T=80K (VI and VII).*

The conductivity switching in our contacts with parallel magnetization of the magnetic nanolayers is more difficult. The conductance switching of the tunnel microcontact $Co_{80}Fe_{20}\uparrow/Pr_6O_{11}/\uparrow Co_{30}Fe_{70}$ of the low-resistance state to the high-resistance state $Co_{80}Fe_{20}\uparrow/Pr_6O_{11}/\downarrow Co_{30}Fe_{70}$ by the action of the laser pulse is only possible under irradiation of this contact in the magnetic field, which is directed antiparallel to the direction of the magnetization of the magnetic layers in the contact. In the contact $Tb_{22}Co_5Fe_{73}\uparrow/Pr_6O_{11}/\uparrow Tb_{19}Co_5Fe_{76}$ is possible to get the decrease of its conductivity without the external magnetic field due to the irradiation of the picosecond or femtosecond laser pulse with circular polarization. The tunnel microcontact $Tb_{22}Co_5Fe_{73}\uparrow/Pr_6O_{11}/\uparrow Tb_{19}Co_5Fe_{76}$ can be switched to the high resistance state without an external magnetic field when it is irradiated by high-power picosecond or femtosecond laser pulse with circular polarization. However, our studies have shown that after irradiation with a powerful laser pulse changes the conductivity of the tunnel barrier of our contacts.

The value of the magnetoresistance (TMR) in a tunnel contact is defined as (TMR) [28]

$$TMR = \frac{R_{\max} - R_{\min}}{R_{\min}}, \qquad (12)$$

where R_{max} and R_{min} are the maximal and minimum values of the resistance. We got value TMR for best samples of contacts $Tb_{22}Co_5Fe_{73}/Pr_6O_{11}/Tb_{19}Co_5Fe_{76}$ TMR>70% at *T=300 K* and TMR>240% at *T=80 K*. For best samples of contacts $Co_{80}Fe_{20}/Pr_6O_{11}/Co_{30}Fe_{70}$ the values of TMR were smaller and reach the values of TMR ≈25% at *T=300 K* and

TMR≈100% at $T=80$ K. The values R_{max}, R_{min} and TMR in our contacts are practically unchanged after a multiple switching of the conductivity in a magnetic field. The resistance of our contacts under the influence of a powerful laser pulse is changed in the transition from a high-resistance state (R_{max} –state) to a low-resistance state (R_{min} –state) is higher than in the same switching in the magnetic field. For the reverse transition from the state R_{min} to the state R_{max} the resistance of our contacts increases under the influence of a single high-power laser pulse is less than in the same switching in the magnetic field. The resulting value the magnetoresistance for such the transition is less than almost (20-30)% than for the same transition in a magnetic field. The value of TMM of our contacts reduced significantly more with the multiple irradiation powerful laser pulses.

The conductivity G of a barrier two-layer magnetic structure depends on the orientation of the magnetization in ferromagnetic layers but also depends on the characteristics of the barrier nanolayer [30]

$$G = \frac{e^2}{h}|T|^2 = A\frac{e^2}{h}\left(1+P^2\cos\theta\right)\exp\left(-2\kappa s\right) \qquad (13)$$

where $P=[N_{\uparrow}(E)-N_{\downarrow}(E)]/[N_{\uparrow}(E)+N_{\downarrow}(E)]$; $\kappa=\sqrt{2m^*(U-E_F)/\hbar^2}$; $N(E)=f(\sigma=\uparrow,\downarrow)$ are the state density on the Fermi level (E_F) for electrons with the spin σ; Θ is angle between the magnetization vectors $\mathbf{M}_1$ and $\mathbf{M}_2$ of two ferromagnetic; e and m^* are the charge and a effective mass of electron; U is a barrier thickness; A is a proportionality coefficient.

Our results show that the irradiation tunnel microcontacts powerful laser pulses causes a change in the characteristics of the barrier layer. This change may be caused by a diffusion of magnetic atoms in the barrier nanolayer as well as changes of the magnetic characteristics of the magnetic layers. Therefore, powerful laser pulses can be used to study dynamics of magnetization reversal of magnetic films, but it is impossible to use such laser pulses to control the conductivity of the magnetic tunnel contacts.

However on the basis of these results we have developed the method of a data recording on a spin storage media [30]. The scheme of such storage spin media and storage cell of this storage media are shown in Figure 7. The electrodes 1, 3 and 4 of this cell should be made of the magnetic material with a high degree of spin polarization of electrons and it should have perpendicular anisotropy or uniaxial planar magnetic anisotropy in the plane. The coercive force H_1 of the first electrode should be bigger than the coercive force H_3 of the third electrode, and the coercive force H_4 of the fourth electrode is bigger than the coercive force of the first electrode: H_1>(1,2-1,4)H_3 and H_4>(1,2-1,3)H_1. Different values of coercive force make it possible to magnetize magnetic electrodes 1 and 4 of our storage cell in the opposite direction by means of external magnetic field.

As the material for barrier nanolayer it is better to use MgO or Pr_6O_{11}. The magnesium oxide has a special electronic structure that provides record high values of tunnel magnetoresistance (TMR>300%) in the tunnel magnetic contacts [22]. The praseodymium oxide is a high energy-gap semiconductor which at the room temperature is in the paramagnetic state. If we place a thin nanolayer Pr_6O_{11} between two ferromagnetic layers the nanolayer Pr_6O_{11}, it is magnetized at the expense of penetration of polarized electrons into it.

Data recording in our cells is carried out by means of powerful electric nanosecond pulses. For data recording in the form of "1" the negative pulse energizes the pair of first-third electrodes, and for data recording in the form of "0" pulse energizes the pair of the fourth-third electrodes. The amplitude U_r and duration τ_i of the electric nanosecond pulses is necessary for defining from the experiments. It should be such that the value of the magnetic field $H_s \sim N\mu_B$ which is created in the electrode 3 by injected polarized spins exceeded the field of anisotropy H_a of the material of this electrode. The value of a spin current j_s is proportional to value of a usual electric current j which is in our tunnel contact $H_s \sim U_r R^{-1} \tau_i^{-1} \tau_s$. Where τ_s – spin polarization relaxation time in electrode 3; μ_B – Bohr magneton. The polarized electrons are injected out of the electrode 1 or out of the electrode 4 to the electrode 3 and create nonequilibrium magnetic field which switches this electrode in the direction of magnetization of the first or the fourth electrode.

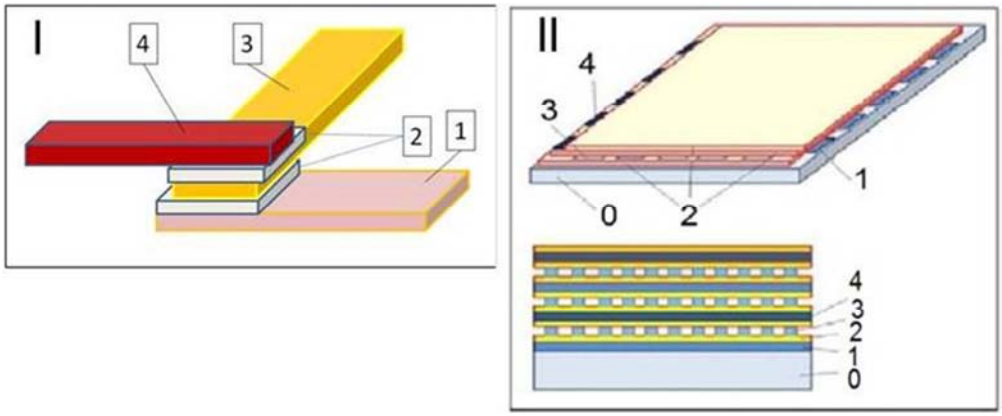

Figure 7. *The scheme of storage cell (I) and storage spin media (II): 0 – substrate, 1 –first magnetic electrode, 2 –barrier nanolayer, 3 –second magnetic electrode, 4 –third magnetic electrode.*

Differential method of reading the information is used in our cell. The differential amplifier registers the electric signal U_i as equal to the difference of conductivity of the tunnel contact 1-3 and the tunnel contact 4-3 $U_i \approx (J_{43} - J_{13})$. The electrode 3 is used as a common electrode. The amplitude of the read pulse must be much smaller than the amplitude of the write pulse. Conductivity of our tunneling contact depends on the relative orientation of the magnetization vectors in the electrodes that contact (13). When "1" is written in our storage cell, we receive the positive value of the electric signal and when "0" is written we receive a negative value of the reading signal. The value of the reading signal was equaled some microvolt at record "1" and at record "0" the value of reading signal was negative and a little smaller.

On the basis of such storage cell it is possible to make a multilayered spin carrier of the information (Fig.5-II). Such spin carrier of the information consists of a system of *klm* storage cell. The very small volume of the storage cell in such spin carrier gives a chance to reach a very high information capacity with the small size of this carrier. In the described spin carrier of information it is possible to make the information record-reading by parallel way that considerably increases the speed of such process.

6. Terahertz Radiation on the Excitonic Transition in CdS Crystals

In this section, we want to inform about the interesting possibility of the creating effective compact sources of terahertz radiation. Interest to electromagnetic radiation in the terahertz frequency range is caused by a wide perspective of its use in biology and medicine, in communications systems. For practical application of terahertz radiation (THR) need compact sources and receivers. Most of the known THR sources have large overall dimensions and low efficiency. The getting THR radiation on transitions between the levels of excitons in semiconductors is in our opinion a promising method for creating THR sources. The energy of these transitions (0,05-0,001 eV) corresponds to the energy TGI, and since excitons are the excited states of the semiconductors, we can get a big coefficient of amplification for the such mechanism of electromagnetic radiation. The getting the population inversion on the excitonic levels is difficult, which is due to the strong exciton-photon interaction and low lifetime of the excited states of the excitons.

A special feature of our work is that the population inversion on the excitonic levels and accordingly the radiation in the terahertz spectral range is achieved by strong exciton-exciton scattering and the generation of visible laser radiation n the band of the exciton-exciton scattering [31].

We used grown from the gas phase thin monocrystalline CdS plate thickness 0,02-0,25 mm. These crystals contain a very small amount of defects, to provide them a high concentration of excitons at a low level of optical excitation. The crystals created by cleaving along the crystallographic axis of the crystal resonator type "without a bottom and the roof of the box." The crystals were irradiated with the Hg-lamp or nanosecond pulses of the N_2 laser at T = 300 K, 77 K and 4 K. The excitation laser pulses cause the generation of visible light at room temperature in crystals that have the crystal resonator. The visible radiation coming out of the four edges of the crystal and the diagram of radiation is in the form of diaphragm blade (7-15 blades). This radiation is the same as the P-band radiation and the spectral position of the irradiation of the generation is in the long-wave part of the broad P-band, which in the literature is due to the radiation processes in the exciton-exciton scattering (Figure 8). Simultaneously with the generation of visible irradiation we recorded radiation in longer wavelengths $\lambda \geq 100\ \mu$. The pulse of this radiation has the longer duration as the pulse of the N_2 laser, but there is a slight delay in time relative to the excitation pulse of this laser. The amplitude long-wave pulse increases almost linearly with the increasing of power of the N_2 laser, while the amplitude of the generation pulse of the visible irradiation increases nonlinearly with the increasing of power of the N_2 laser. This long-wave pulse has the asymmetrical temporary form with a steep leading edge of a pulse and a longer edge of recession.

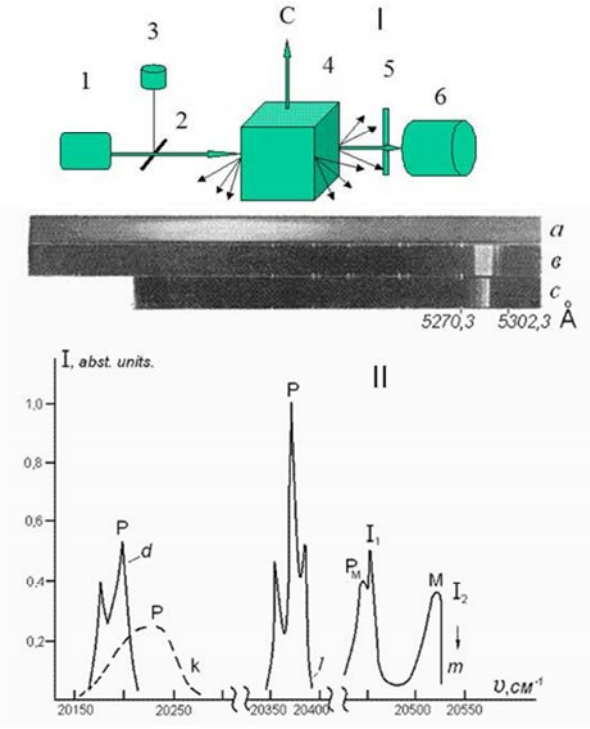

Figure 8. *The optical scheme of the experiment*

(I) and emission spectra of CdS crystal (II): I-1 – N_2 laser, I-2 – plate, I-3 – photodiode, I-4 –CdS crystal, I-5 – filter, I-6 –pyroelectric detector; *a*, *k* and *m* – the spontaneous radiation and the crystal resonator offline, *b*, *c* and *d* – the radiation in crystals with the resonator and the generation of radiation in the P-band; *a*, *b* and *c* – T= 300 K; *k* and, *d* –T=77 K; *l* and *m* – T=1.4 K;

The spectral composition and the dynamics of the long-wave radiation gives us reason to believe that we recorded terahertz radiation, which arises due to transitions of excitons with a high energy level to a lower energy level. The intensity of radiation of P-band should be proportional to the square of the average concentration of the excitons N, when there is no light generation in this band. The exciton-excitonic scattering leads to an increase in the concentration of excitons at all excitonic levels j = n≥ 2,3, as evidenced by the large width of P-band. The concentration of excitons N_j on the j level can be found from the expression

$$N_j \approx A_j N_0^{\,2} f(E_{ex})\delta(E_j - E_{ex-ex})\sigma\tau_j \approx A_j \frac{4\pi^2 I^2 \alpha^2 (1-R)^2 \sigma\tau_0^{\,2}\tau_j}{h^2\omega^2}\delta(E_j - E_{ex-ex}) \quad (14)$$

In the generation in the P-band increases the efficiency of exciton transitions for a certain j level, which is determined by the wave radiation length of the generation. In the first approximation concentration of excitons at this level can be found from the following expression

$$N_i(J_i) \approx A_i\gamma_i J_i N_0^{\,2}\sigma \approx A_i\gamma_i \frac{16\pi^4 I^4\alpha^4(1-R)^4\sigma^2\tau_0^{\,4}\tau_i}{h^4\omega^4} \quad (15)$$

where I, ω, R and α is the intensity, frequency, coefficient of reflection and coefficient of absorption of the laser radiation; $\sigma \approx B\pi r_{ex}^{\,2}\upsilon_{ex}$ – cross section of the scattering of excitons, τ is the lifetime of excitons; r_{ex} and υ_{ex} is the range and mean velocity of the exciton; h is Planck's constant;, γ_i is proportionality coefficient, which characterizes the efficiency of stimulated luminescence and its value depends on the quality factor of the resonator; A is proportionality coefficient. Therefore, the concentration of excitons at the *i* -level can be much greater than the concentration of excitons at lower energy levels. The ratio of the concentration of excitons at the *i*-level to the concentration of excitons at a lower *k*-level to be defined as

$$\frac{N_i}{N_k} \approx \frac{A_i\gamma_i J_i N_1^{\,2}\sigma\tau_i}{N_1\exp(-\Delta E_{1k}/kT)} \approx A_i\gamma_i \frac{8\pi^3 I^3\alpha^3(1-R)^3\sigma^2\tau_1^{\,3}\tau_i}{h^3\omega^3\exp(-\Delta E_{1k}/kT)}, \quad (16)$$

where ΔE_{1k} – the energy difference between the first and the *k*-level.

Estimation of the population inversion for our experimental conditions, shows that the concentration of excitons at the *i*-level higher than the concentration of excitons, even at the first level. If the *k*-level to consider the second and third level, then we obtain from (16) the very large values of the ratios of concentrations of the excitons. The results of our research show that in the thin ideal CdS single crystals can be obtained on the population inversion of the exciton levels and thus obtain stimulated emission of electromagnetic radiation in the terahertz frequency range.

Analysis of the interaction of laser radiation with thin films indicates good prospects the use of laser radiation to dope thin films to improve the surface characteristics of metal materials and to improve magnetic characteristics and dynamics of the magnetization of the magnetic films.

References

[1] M. K. El-Adawi, S. A. Shalaby, S. E. S. Abdel-Ghany, (2015), Interaction of Laser Radiation with Solids, International Journal of Natural Sciences Research, , Vol. 3, No. 6, pp. 83-100.

[2] Femtosecond-Scale Optics, (2011), Ed. A. V. Andreev, Publisher: InTech, Chapters, p. 446.

[3] A. M. Danishevskii, A. A. Kastalskii, S. M. Ryvkin, and I. D. Yaroshetskii, (1970) Photon drag effect of the free carriers in direct interband transitions in semiconductors, Sov. Phys. JETP, Vol. 31, pp. 292-297.

[4] A. F. Gibson, M. F. Kimmitt, and A. C. Walker, (1970), Photon drag in Germanium, Appl. Phys. Lett., Vol. 17, pp. 75-79.

[5] A. Ashkin, (1972), The pressure of laser light, Scientific American, Vol. 226, No. 2, pp.63-71.

[6] W. D. Phillips, (1998), Laser cooling and trapping of neutral atoms, Rev. Mod. Phys., Vol. 70, No. 3, pp. 721-741.

[7] F. H. Gelmuhanov, A. M. Shalagin, (1979). Light-induced diffusion of gases, Sov. JETF Letters, Vol. 29, pp.773-776.

[8] H. Ohno, (1998), Making Nonmagnetic Semiconductors Ferromagnetic, Science, vol. 281, pp. 951–956.

[9] J. Cibert, J. Bobo, U. Lüders, (2005) Development of new materials for spintronics, Comptes Rendus Physique, Vol. 6, pp. 977-996.

[10] H. Raether, (1986), Surface plasmons on smooth and rough surfaces and on gratings, Heidelberg, Springer-Verlag, p.136.

[11] E. G. Bortchagovsky, S. Klein, U. C. Fischer, (2009), Surface plasmon mediated tip enhanced Raman scattering, Appl. Phys. Lett., Vol. 94, pp.063118-06321.

[12] G. A. Askaryan, M. C. Rabiovych, A. D. Smirnova and V. B. Studentov, (1967), The currents generated in the material by radiation pressure of the laser beam, Sov. JETF Letters, Vol. 5, pp. 116-118.

[13] M. M. Krupa, (2001), Light induced drift electrons in thin magnetic films, JETPh, Vol. 120, No.11, pp. 10-15.

[14] A. Yu. Bonchika, S. G. Kijak, Z. Gotrab,W. Proszakc, (2001), Laser technology for submicron-doped layers formation in semiconductors, Optics & Laser Technology, Vol. 33, pp. 589-591.

[15] W. Kautek, P. Rudolph, G. Daminelli and J. Krüger, (2005), Physico-chemical aspects of femtosecond-pulse-laser-induced surface nanostructures, Appl. Phys. A, Vol. 81, No. 1, pp. 65-70.

[16] M. M. Krupa, Yu. B. Skirta, (2006), Drift of atoms of bismuth in the field of laser radiation and a data recording in thin films phthalocyanine dye, Radiophysic and Quantum Electronic, Vol. XLIX, No. 6, pp. 513-518.

[17] R. Merservey, P. M. Tedrov, (1994), Spin-Polarized Electron Tunneling, Phys. Rep., Vol. 238, No. 4, pp. 175-239.

[18] M. M. Krupa, A. M. Korostil, (2007), Impact of laser irradiation on magneto-optical properties of multilayered film structures, Inter. Journal of Modern Physics B, Vol. 21, No. 32, pp. 5339-5350.

[19] M. Komori, T. Nukata, K. Tsutsumi, C. Inokyti, I. Sakyrai, (1984), Amorphous TbFe Films for Magnetic Printing with Laser Writing, IEEE Trans. Magnetic, Vol. 20, No. 5, pp. 1042-1044.

[20] A. V. Kimel, B. A. Ivanov, R. V. Pisarev, P. A. Usachev, A. Kirilyuk, Th. Rasing, (209), Inertia-driven spin switching in antiferromagnets, Nature Physics, vol. 5, pp. 727-731.

[21] T. A. Ostler, J. Barker, R. F. Evans, et al., (2012), Ultrafast heating as a sufficient stimulus for magnetization reversal in a ferrimagnet," Nature Communications, No. 3, pp.1-6.

[22] R. Pittini, P. Wachter, (1998), Cerium compounds: The new generation magneto-optical Kerr rotators with unprecedented large figure of merit, JMMM, Vol. 186, No. 3, pp. 306-312.

[23] R. Hertel, (2006), Theory of Optical Rotation, Faraday Effect, and Inverse Faraday Effect, Journal of Magnetism and Magnetic Materials, Vol. 303, pp. L1–L4.

[24] J. C. Slonczewski, (1996), Current-driven excitation of magnetic multilayers, Journal of Magnetism and Magnetic Materials, Vol. 159, pp. L1-L7.

[25] M. M. Krupa, (2013), Switching of Magnetic Films by Femtosecond Laser Pulses and Control Spin Current, Advances in Optoelectronic Materials, Vol. 1 No. 3, pp. 48-58.

[26] M. M. Krupa, (2008), Spindependent tunnel conductivity in films TbCoFe/Pr_6O_{11}/TbCoFe. JETPh Letters Vol. 87, No. 10, p.p. 635-637.

[27] J. Katine, F. Albert, R. Buhrman E. B. Myers and D. C. Ralph., (2000), Current-Driven Magnetization Reversal and Spin-Wave Excitations in Co/Cu /Co Pillar, Phys. Rev. Letters, Vol. 84, pp. 3149–3152.

[28] M. Julliere, (1975), Tunneling between ferromagnetic films, Phys. Letter., Vol. 54, No. 3, pp. 225-226.

[29] I. Zuti´c, J. Fabian, and S. Das Sarma, (2004), Spintronics: Fundamentals and Applications, Rev. Mod. Phys., Vol. 76, No. 2, pp. 323-410.

[30] M. M. Krupa, (2014), Patent of Ukraine 19 UA 106260 Method of a magnetic recording of the information and a magnetic spin data carrier. Publ11.08.2014, bull. №15.

[31] M. M. Krupa, (2009), Patent 19 UA №86248 19UA Ukraine, The device for laser terrahertz generation. Publ 10.04. 2009, bull. №7.